

Chapter 5

**Western Arabian Sea: SW Monsoon
History since the Last Glacial Maximum**

5.1. Introduction:

The western Arabian Sea is best suited to study the past variations of monsoon, as it experiences intense upwelling during the SW monsoon (Wrytki, 1973; Shi et al, 2000). The upwelling brings up nutrient rich, cold water from deeper levels of the ocean to the sea surface. This causes enhanced productivity (Kabanova, 1968; Codispoti, 1991) and reduces the sea surface temperature by at least 4°C (Haake et al, 1993 a, b). This provides the largest detectable signal for studying the paleomonsoon variations. No wonder a large number of earlier studies are concentrated in this region (Prell et al, 1980; Prell and Kutzbach, 1987; Clemens et al, 1991; Anderson and Prell, 1993; Sirocko et al, 1993; Naidu et al, 1993; Naidu and Malmgren, 1995; Reichert et al, 1997, 1998; Schulz et al, 1998; Anderson et al, 2002; Gupta et al, 2003). We obtained a core SS 4018 G from the western Arabian Sea near the mouth of the Gulf of Aden. The base of the core corresponds to a period when the earth had already experienced the most severe glaciation and was recovering towards a warmer climate. But starting from 15 ka BP to 10 ka BP, the earth's climate fluctuated between extremes that plunged back the earth into the cold, comparable to that of the Last Glacial Maximum, and pulled it out as suddenly to the balmy conditions akin to today. These rapid climate changes took place in a matter of few decades to few centuries. It becomes necessary to assess the behavior of the monsoon during such extreme climatic changes. Furthermore, the variations exhibited by SW monsoon during the Holocene (past 10,000 years) is a matter of debate with some workers favouring decreased monsoon intensity during the Holocene (Gupta et al, 2003; Sirocko et al, 1993) whereas others demonstrating an increasing monsoon for the major part of the Holocene (Agnihotri et al, 2003; Sarkar et al, 2000). This study is based on a large number of AMS radiocarbon dates on planktic foraminiferal separates, and multi-proxy isotopic and chemical analysis of the core will help to resolve this problem.

5.2. Core location:

The core is located at the mouth of the Gulf of Aden near the Red Sea in the Western Arabian Sea. It has been raised from a water depth of 2830 m, which is well above the lysocline in the Western Arabian Sea (~3900 m, Kolla et al, 1976). Refer

Table 2.1 for additional details. Core location is shown in Fig. 5.1 along with other cores with which this study has been compared.

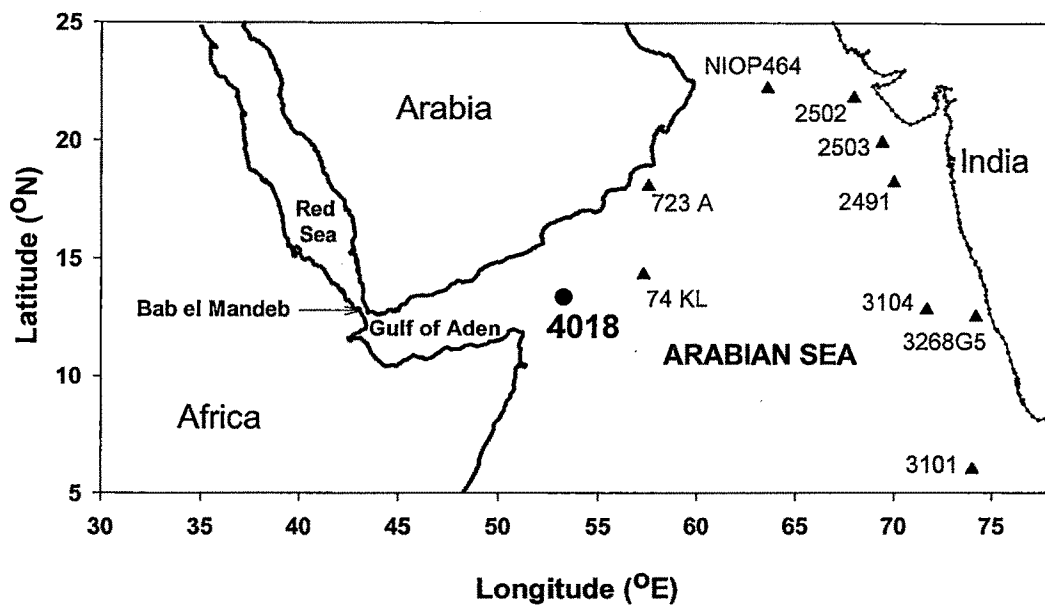


Fig 5.1. Locations of the Core SS 4018G (this study, shown by circle) and other cores with which it has been compared (depicted by triangles)

5.3. Oceanographic conditions at the core site:

There are three kinds of water masses that can be distinguished in the Arabian Sea *viz.* those generated by downwelling, those that are mixtures of other water masses and those that enter from outside. Two shallow subsurface water masses that are present just below the monsoon controlled surface mixed layer and formed due to subduction are Arabian Sea Water (ASW) and Subtropical Subsurface water (SSW) (Schott and McCreary Jr., 2001). ASW or Arabian Sea High-Salinity Water forms in the northern Arabian Sea due to winter cooling during the North East monsoon and spreads southward (Morrison, 1997; Schott and Fischer, 2000) just below the surface layer and upto 100m water depth (Prasanna Kumar and Prasad, 1999). SSW forms in the subtropical gyre of the southern hemisphere as a high salinity water due to excess of evaporation over precipitation. It joins the westward flowing South Equatorial Current (SEC) at 200-250 m water depth and it shoals to 100 m by the time it reaches the

western boundary (Swallow et al, 1988). Thereafter it spreads northward across the equator with the Somali Current, ultimately participating in supplying water to the upwelling off Somalian and Arabian coast (Schott and McCreary Jr., 2001). Another set of high salinity subsurface waters is Persian Gulf Water (PGW) and Red Sea Water (RSW). Persian Gulf Water is a saline water mass that originates due excess of evaporation in the Persian Gulf and enters the Arabian Sea through the Strait of Homruz. It is found at a depth of 200 - 400 m and does not extend far beyond the northern Arabian Sea (Rhein et al, 1997; Prasanna Kumar and Prasad, 1999). Red Sea Water originates in the northern part of the Red Sea and advects into the Arabian Sea through the Strait of Bab el Mandeb as highly saline and warm water mass (Maillard and Soliman, 1986; Woelk and Quadfasel, 1996). RSW occurs at a depth of 100 – 150 m at the Bab el Mandeb and downstream it mixes strongly with the surrounding waters and by the time it reaches Somalian coast off Socotra it sinks to ~800 m water depth (Shapiro and Meschanov, 1991; Woelk and Quadfasel, 1996).

At intermediate depth is found the Antarctic Intermediate Water (AAIW) that enters the basin through the southeastern region (Fine, 1993). It is formed at the subpolar frontal zone and is marked by low salinities because of excess of precipitation over evaporation over there (Schott and McCreary, 2001). The IDW or Indian Deep Water that is specific to northern Indian Ocean occupies the greatest depths. It flows in the density range just above the Circum Polar Deep Water (CDW), and is presumably generated by deep upwelling out of CDW (Mantyla and Reid, 1995).

The surface circulation at the core site is controlled by the seasonal reversal of monsoonal winds. Refer to Figs.1.1 and 1.2 for schematic diagrams of the Indian Ocean circulation during the summer and winter monsoons respectively. The Southeast Trade winds drive the westward flowing South Equatorial Current (SEC) in the latitude range 17 - 22⁰S. At the tip of Northern Madagascar, about 17⁰S, SEC splits into two parts that flows northwards and southwards and are called as Northeast Madagascar Current (NEMC) and Southeast Madagascar Current (SEMC). NEMC feeds the northerly flowing East African Coast Current (EACC, Schott and McCreary Jr., 2001). During the summer monsoon the EACC feeds the northward flowing

Somali Current (SC) that develops into various clockwise rotating cells and gyres such as Southern Gyre (SG), Great Whirl (GW) and Socotra Eddy (SE) that develops northeast of Socotra Island (Fig.1.1) (Schott et al, 1990; Brock et al, 1991). It induces intense upwelling along the Somalian and Oman coast with upwelling velocities close to 3×10^{-3} cm/sec and an upwelling transport of 1.5 – 2 Sv in the upper 50 m as shown in the Fig. 5.2 (Smith and Bottero, 1977; Shi et al, 2000).

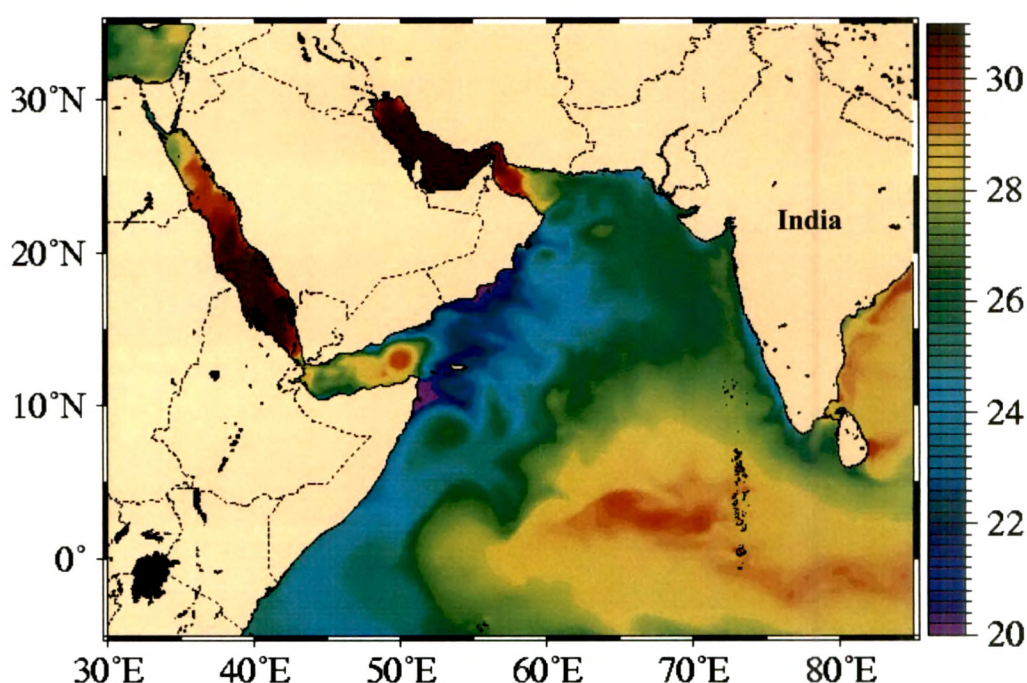


Fig.5.2. SST contours (in $^{\circ}\text{C}$) during August. The upwelling along the Somali and Oman coast is manifested by the reduction in SST due to surfacing of cooler waters from below.

The typical temperature of the upwelled water is $19 - 24^{\circ}\text{C}$ (Schott and McCreary Jr., 2001). The reasons attributed for such intense coastal upwelling is the Ekman divergence due to the flow of strong winds parallel to the coast. As the surface water moves away from the coast, water from below upwells to take its place. The offshore upwelling takes place due to the strong positive wind stress curl to the NW of the axis of the Somali jet, which is a low level cross-equatorial jet (Smith and Bottero, 1977; Shallow, 1984). The central Arabian Sea exhibits a bowl shaped mixed

layer deepening under the effect of Findlater Jet wind-stress forcing and Ekman pumping (McCreary and Kundu, 1989; Rao and Sivakumar, 2000).

During the winter monsoon, the Somali Current reverses its direction and flows southward and meets the EACC at 2-4°S that supplies the eastward flowing South Equatorial Countercurrent (SECC, Dueing and Schott, 1978; Swallow et al, 1991). The cold and dry Northeast monsoon winds accompanied by the Ekman pumping cause subduction of the high salinity surface waters in the northern Arabian Sea (Morrison, 1997; Schott and Fischer, 2000).

5.4. Age – Depth model:

SS 4018G has 15 radiocarbon dates of planktonic foraminiferal separates (see section 2.3). One depth viz. 60 - 62 cm was repeated by picking another set of planktic foraminifera and both the samples gave similar result. For this particular sample the two radiocarbon dates obtained are 10364 ± 55 and 10543 ± 60 , which after calibration gave the calendar ages as $11,000 \pm 230$ and $10,930 \pm 380$ respectively that are similar within the error range (errors given are 1 standard deviation). An average of both the values i.e. 10965 ± 222 has been taken for the Age – Depth model. This core covers up to ~19,000 calendar years (depth~130cm) and thus possess an average sedimentation rate of $\sim 7\text{cm}/10^3$ years. Although this core is from an open ocean location (water depth: 2830m), it has a high sedimentation rate owing to the high surface productivity. The resolution in this case is 150 years per cm but since the sampling is done at every two cm, the effective resolution becomes ~ 300 years per sample. For the dates in tabular form and other related information, please refer to the Table 2.2.

The radiocarbon dates in this core has been calibrated to calendar ages using the calibration program “Calib 4.1 (INTCAL 98)” (Stuiver et al, 1998) with a reservoir age correction of 563 ± 30 years ($\Delta R = 163 \pm 30$ yr, Dutta et al, 2001). Recently Southon et al (2002) carried out extensive study in the Indian Ocean regarding the oceanic reservoir ages. For the western Arabian Sea they proposed a mean ΔR value of 190 ± 25 yr that is very similar to that of Dutta et al (2001). The Age-Depth model is shown in the Fig.5.3.

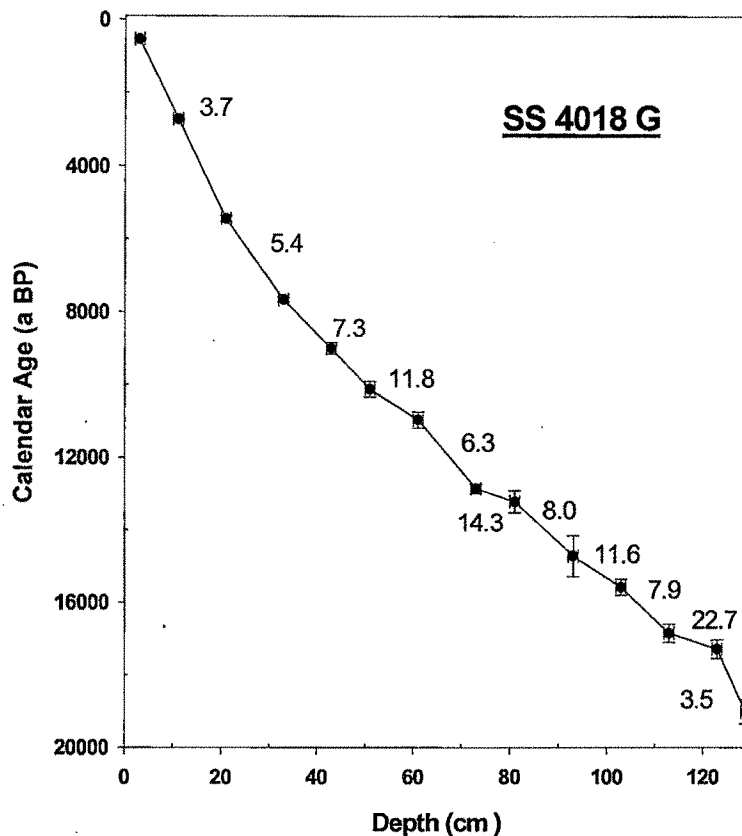


Fig. 5.3. Calibrated radiocarbon ages and sedimentation rates (cm/kyr) for SS4018G.

5.4. Downcore productivity variations in the core SS 4018 G:

Oceanic productivity manifests itself in many forms such as calcareous (foraminifera, coccoliths, pteropods), siliceous (diatoms, radiolarians) and organic productivity. To determine the productivity variation in SS4018 G, various chemical proxies (i.e. CaCO_3 %, C_{org} %) and isotopic proxies (i.e. $\delta^{15}\text{N}$, $\delta^{13}\text{C}$) were measured.

5.4.1. Productivity as manifested by CaCO_3 and C_{org} :

Calcareous productivity (CaCO_3 wt. %) can be taken as an indicator of overhead productivity if the core has been raised above the lysocline and has not

suffered any carbonate dissolution. Moreover it should not have been diluted by the terrestrial input (Sirocko et al, 1993, Naidu et al, 1993). Similarly organic productivity as exhibited by the C_{org} (wt. %) can point towards past productivity variations provided it has not been contaminated by terrestrial organic matter, or wasn't oxidized by oxic bottom waters.

Organic carbon preservation is controlled by the availability of the oxidizing agents and its removal from the diagenetically active layer with complex interplay of many variables such as organic matter composition, bioturbation rates, diffusive openness of the sediments to various oxidizing agents and protective adsorption of organic matter on the mineral surfaces etc. (Hedges and Kiel, 1995). The core has been raised from a water depth of 2830m that is overlain by oxic waters. But the core site experiences high sedimentation rate (~7 cm/kyr) due to the intense productivity occurring over there (Nair et al, 1989). Due to the high sedimentation rate the organic matter rapidly crosses the diagenetically active layer, which is of the order of ~20 cm. Thus the organic matter not only escapes the effect of bioturbation that is more active near the sediment surface but also the dissolved oxidizing agents such as O_2 , NO_3^- , SO_4^{2-} etc. (Heinrichs, 1992). Furthermore several workers have questioned the effect of oxygen availability on diagenesis. Several laboratory and field studies of the relative mineralization rates of bulk organic matter or specific biochemical compounds such as dissolved sugars, amino acids etc. under oxic vs. anoxic conditions have indicated little or no effect of O_2 concentration (Foree and McCarty, 1970; Hansen and Blackburn, 1991; Cowie and Hedges, 1991,1992; Lee, 1992; Hedges and Kiel, 1995). Moreover lack of any relationship between sedimentary organic matter preservation and O_2 concentrations (Pederson et al, 1992; Calvert and Pederson, 1992) or burial efficiencies (Heinrichs and Reeburgh, 1987; Betts and Holland, 1991) has cast doubts on the importance attached to the oxygen availability. Thus many exceptions exist to the oxygen effect and there is no universal pattern (Pederson et al, 1992).

Schulte et al (1999) carried out multi-proxy study on a core near [Maldives raised from a water depth of 2450 m] that has experienced oxic conditions throughout its history. They have conclusively proved that the variation in organic carbon is due to overhead productivity alone and is not affected by the bottom water preservation

characteristics. Similarly Reichart et al (1997) studied a core from the Murray Ridge in the Northern Arabian Sea from a water depth of 1470m (oxic waters) and concluded that C_{org} record is a manifestation of surface water productivity.

Rostek et al (1997) obtained a core from a location adjacent to that of SS4018 G from a water depth of 2490 m. The similar variations exhibited by C_{org} and total alkenone concentration proved that variations in organic matter are related to marine productivity. Following figure shows the downcore variation in the $CaCO_3$ (wt. %) and C_{org} (wt. %) that are controlled mainly by the overhead productivity changes.

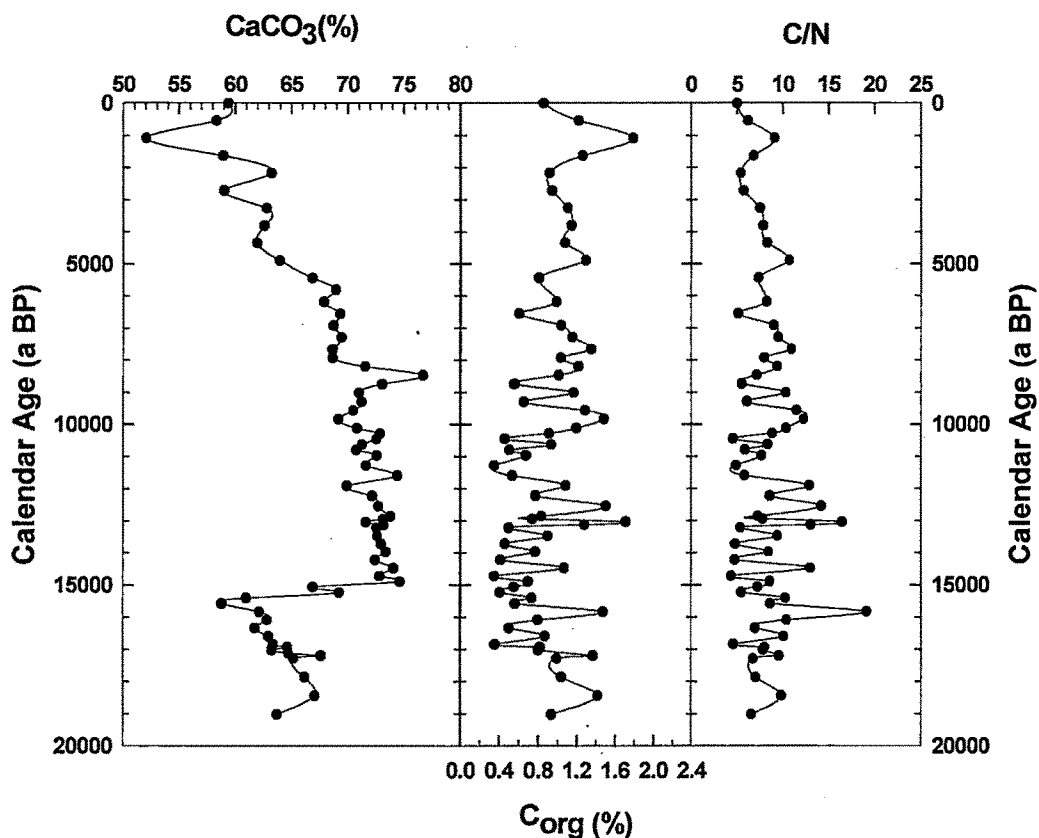


Fig. 5.4. Downcore variations of productivity proxies in the core SS 4018 G

C/N ratio indicates the provenance of the organic matter: recent marine sedimentary organic matter has a typical value of $\sim 8 \pm 2$ and older sediments yield organic matter with a value of ~ 12 to ~ 15 (Mackenzie, 1980). In contrast, the terrestrial organic matter has a C/N ratio of ~ 20 to ~ 100 with an average value of ~ 60

(Premuzic et al, 1982; Meyers, 1994). In this core, the average C/N value is ~9. Prior to Holocene there are some variations but the values still fall well within the range for marine organic matter. Thus the C/N values in this core unequivocally point towards the marine origin of the organic matter with negligible terrestrial input, if any.

The calcareous productivity as evident by the CaCO_3 (wt. %), and the organic productivity (C_{org}) show a decreasing trend upto 15 ka BP indicating a reduced monsoon during the early deglacial period. Thereafter calcareous productivity exhibits an enhancement at 15 ka BP pointing towards an increase in the monsoon intensity that coincides with the major deglaciation episode. Albedo changes associated with melting of Tibetan glaciers (Zahn, 1994) can cause more heating of the Tibetan plateau that can lead to an enhanced monsoon. After 15 ka BP, the CaCO_3 productivity stays more or less uniform upto 9 ka BP where it shows a sudden increase indicating monsoon enhancement. This episode of monsoon enhancement follows just after the maximum summer insolation in the latitude 20°N to 35°N at 10 ka BP (Loutre et al, 1992). Thereafter the calcareous productivity stays uniform upto 6 ka BP after which it shows a decreasing trend. Such a trend was also seen by Sirocko et al (1993) and Gupta et al (2003) in the cores 74 KL and 723A respectively from the nearby regions (Fig.5.1). Sirocko et al (1993) also observed an increase in the monsoon intensity at ~15 ka BP as evident by the increased calcareous productivity at that time and an enhancement at ~9 ka BP. Thereafter they found a decreasing trend in the calcareous productivity which they attributed to the decreasing monsoon intensity during the Holocene (past 10,000 years). Similarly, Gupta et al (2003) have analyzed *G.bulloides* % in the core 723A covering the Holocene. *Globigerina bulloides* is foraminiferal species inhabiting the temperate to sub-polar waters. It occurs in the tropical regions where upwelling takes place due to which cooler water from the deeper levels surfaces. Thus it is an indicator of upwelling, which in turn is governed by the wind strength. More the *G.bulloides* %, more the wind strength. They found a decreasing *G.bulloides* % during the Holocene that they attributed to a weakening wind strength and hence decreasing monsoon intensity. Recently Fleitmann et al (2003) measured $\delta^{18}\text{O}$ in cave stalagmite from southern Oman and attributed its variation to local precipitation changes. They found a sudden increase in precipitation centered at ~10 ka BP and thereafter a high monsoon

precipitation from 9.6 to 5.5 ka BP. Furthermore they maintain that a long term gradual decrease in monsoon precipitation has taken place from ~8 ka BP to 2.7 ka BP after which there is a hiatus in stalagmite deposition.

But the major limitation of these studies was that they were based on a single proxy. When multiple proxies are taken into account then they point towards a different picture. In the present study CaCO_3 % shows a decreasing trend after 8 ka BP (see Fig.5.3). Had this decrease been due to decreasing monsoon and therefore productivity, then C_{org} should also have shown a decrease as it is manifestation of organic productivity. But such a decrease is not seen, which indicates that productivity probably hasn't decreased during the Holocene. This is further supported by the $\delta^{13}\text{C}$, $\delta^{15}\text{N}$ studies carried out on this core.

5.4.2. Productivity as manifested by $\delta^{13}\text{C}$:

Downcore variations in the $\delta^{13}\text{C}$ in the three species of foraminifera viz. *G.ruber*, *G.sacculifer* and *G.menardii* are shown below in Fig.5.4.

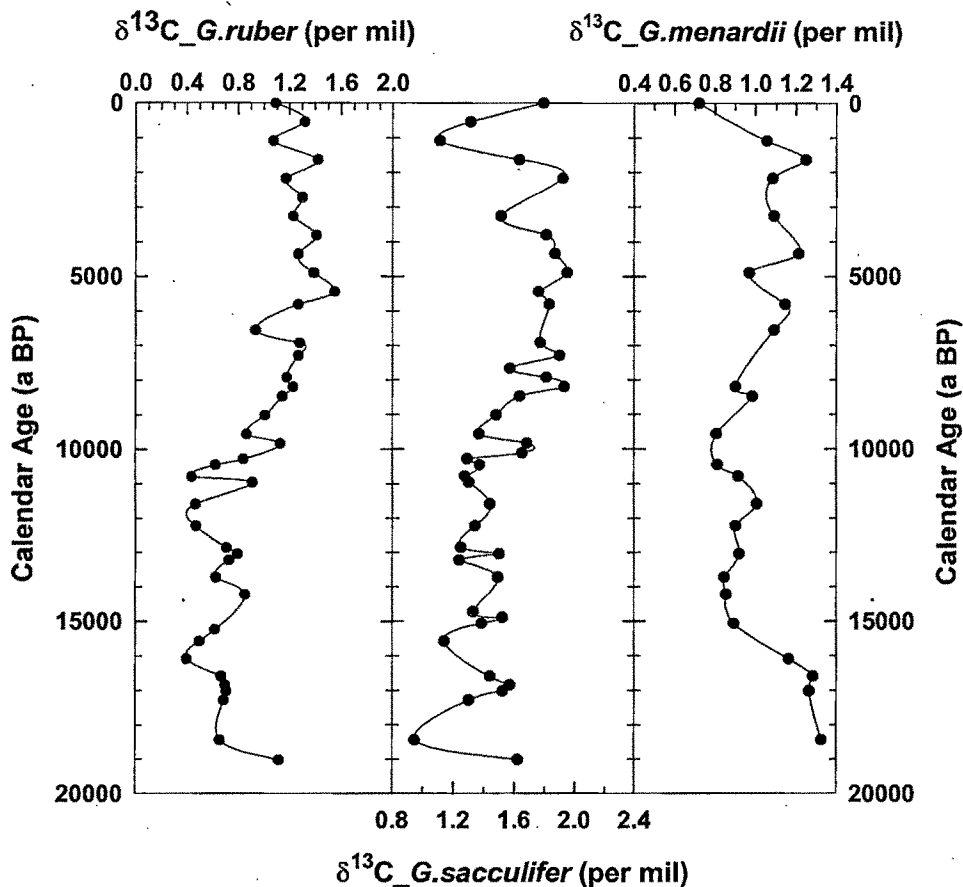


Fig.5.5. Downcore variation of $\delta^{13}\text{C}$ of three species of foraminifera

$\delta^{13}\text{C}$ of calcareous shells of foraminifera are controlled by the carbon isotopic composition of the ambient bicarbonate that in turn is controlled by the organic productivity as discussed in section 2.4.2. During enhanced organic productivity, more of lighter isotope (^{12}C) is taken through photosynthesis, making the calcifying microenvironment enriched in the heavier isotope (^{13}C), the signature of which gets preserved in the calcitic shells of foraminifera. Thus higher $\delta^{13}\text{C}$ in several species indicate enhanced organic productivity. During the Holocene productivity has shown a sharp increase from 10 ka BP to 6 ka BP and thereafter it stays more or less uniform

as evident by the $\delta^{13}\text{C}$ plot of all the three species of the foraminifera. This shows that productivity probably did not decrease during Holocene as hypothesized by earlier workers. It is further supported by the $\delta^{15}\text{N}$ of the sedimentary organic matter.

5.4.3. Productivity as manifested by $\delta^{15}\text{N}$:

The Fig 5.5 shows the downcore variation in the productivity as exhibited by $\delta^{15}\text{N}$ of sedimentary organic matter.

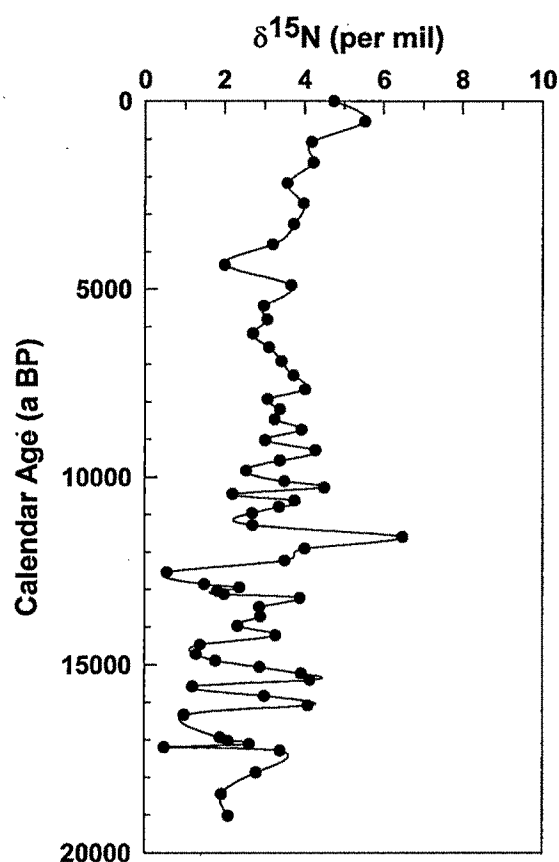


Fig. 5.6. Plot showing the downcore variation of $\delta^{15}\text{N}$ of the sedimentary organic matter in the core SS4018 G

$\delta^{15}\text{N}$ of sedimentary organic matter reflects the surface productivity and the ensuing oxygen depleted conditions as discussed in the section 2.4.3. Higher $\delta^{15}\text{N}$ in general indicates a higher productivity. As evident from Fig.5.5, productivity does not decrease during the Holocene, as revealed by slightly increasing trend seen in $\delta^{15}\text{N}$.

Thus it is apparent that proxies that are manifestation of organic productivity stay more or less uniform or exhibit a slightly increasing trend. This trend in productivity as exhibited by various proxies indicates that monsoon strength did not

decrease during the Holocene. An increase in the monsoon intensity during the Holocene (10 ka –2 ka BP) has also been observed by Agnihotri et al (2003b), Bhushan et al (2001) and Sarkar et al (2000) based on the cores obtained from the eastern continental margin of the Arabian Sea off the western Indian Coast (see Fig. 5.1). But the calcareous productivity in the western Arabian Sea shows a decreasing trend during the Holocene. One way to reconcile these contradictory observations is that increasing monsoon strength favours silicate rather than carbonate production (Naidu et al, 1993; Rixen et al, 1996) and causes cross equatorial transport of the nutrient poor water (Rixen et al, 1996) along the Somali current (Dueing et al, 1980; Schott and Fieux, 1985), which causes further reduction in the productivity.

Haake et al (1993) have shown on the basis of sediment trap data from the Western Arabian Sea that there is enhanced concentration of nitrate and phosphate at around ~30 m water depth, whereas silicate concentration peaks at around ~150 m. During the onset of monsoon, when the monsoon winds just begin to strengthen, upwelling takes place from shallower a depth that enhances the calcareous productivity. But during later stages, as the monsoon wind strength increases upwelling starts from the deeper levels as evident by a further decrease of SST. This injects sufficient silicate into the euphotic zone that leads to diatom blooms causing high siliceous fluxes in the western Arabian Sea (Rixen et al, 1996). Lower sea surface temperatures are associated with high nutrient concentrations (Smith, 1982) that favours diatom blooms (Deuser and Ross, 1980; Deuser et al, 1981). Satellite observations have also shown that plankton blooms that cover the whole northwestern Arabian Sea during the later stages of the SW monsoon (Brock et al, 1991; Brock and McClain, 1992) are diatomaceous (Rixen et al, 1996). Thus it is clear from the above-mentioned observations that increased wind strengths likely lead to enhanced siliceous productivity, rather than calcareous productivity.

Naidu et al (1993) found in a sediment core from the western equatorial Indian Ocean (Somali basin) that $\delta^{13}\text{C}$ of *G. menardii* exhibits enriched values (indicating enhanced organic productivity) in contrast to CaCO_3 % that shows lower values (indicating reduced calcareous productivity) during interglacials. The SW monsoon enhanced during interglacials (Prell and Van Campo, 1986; Clemens et al, 1991) that would have caused increased wind induced surface mixing resulting in higher

productivity. They proposed that the observed anticorrelation between the $\delta^{13}\text{C}$ and CaCO_3 is because of higher biogenic siliceous productivity. Murray and Prell (1991) have also reported higher opal content during interglacials pertaining to increased productivity due to upwelling changes. Naidu et al (1993) further maintain that increased biogenic productivity during interglacials would result in more organic matter degradation that will ultimately cause more CO_2 supply to the bottom waters resulting in enhanced dissolution of CaCO_3 . Similarly Reichart et al (1997) analyzed a core from the northern Arabian Sea namely NIOP464 (shown in Fig. 5.1) covering the past 225 ka and found that high calcareous productivity does not always correspond to enhanced surface productivity as evident by other productivity indicators such as C_{org} . They argued that pelagic carbonate production (including planktonic foraminifera) decreased and was replaced by organic walled and siliceous organisms during enhanced productivity. Enhanced productivity also results in enhanced dissolution of calcite but signs of dissolution such as broken planktonic foraminiferal shells were not found, which implies that the lower CaCO_3 along with high C_{org} is likely due to enhanced siliceous productivity during intense monsoon. The sediments underlying such regions are enriched in silica and organic carbon (Broecker and Peng, 1982) and depleted in calcite. Thus biogenic calcareous productivity might reduce during increased monsoonal wind strengths and is compensated by enhanced biogenic siliceous productivity.

Thus organic productivity has not decreased during the Holocene or at best, has shown a slight increase. But a clear-cut increasing trend is not visible in the productivity proxies. Rixen et al, 1996 observed that during one of the years with the highest monsoon wind strength and minimum SST, the surface productivity was minimum. They attributed this to enhanced cross-equatorial transport of the cold, nutrient poor surface water along the Somali Current. Conkright et al (1994) have shown that waters south of equator are deficient in nutrients as compared to Arabian Sea. The Somali current carries with it the south equatorial waters into the Arabian Sea (Dueing et al, 1980; Schott, 1983; Schott and Fieux, 1985). It flows between the Somalia and Socotra into the upwelling regime off Oman (Fischer et al, 1996). The collapse of the two gyre system (i.e. great whirl and southern gyre) in the later stages of SW monsoon (Evans and Brown, 1981; Schott, 1983) could further strengthen the

cross-equatorial transport along the Somali Current and will control the productivity in the western Arabian Sea. Rixen et al (1996) have proposed that this transport of cold, nutrient poor water is enhanced during higher wind strengths. Such a process could be assumed to take place during the past as well. After the well documented monsoon enhancement at ~9 ka BP, the monsoon strength further increased as evident from the productivity variations in the core SS4018. This further enhancement not only intensified upwelling of nutrient rich waters but also caused increased cross-equatorial transport of nutrient poor waters. These two counterbalancing processes are responsible for the more or less uniform trend seen in various productivity proxies during the Holocene. Monsoon intensification during the Holocene is also supported by the oxygen isotopic analysis as discussed below.

5.5. Oxygen isotopic analysis:

Oxygen isotopic analysis has been carried out on three species of planktonic foraminifera viz. *Globigerinoides ruber*, *Globigerinoides sacculifer*, *Globorotalia menardii* in the core SS4018. *G. ruber* and *G. sacculifer* are surface dwelling species predominantly inhabiting the top ~25m and ~50m respectively. *G. menardii* is a deeper dwelling species found at the top of thermocline at a water depth of 100-150m (Be, 1977). Fig.5.6 (please see the next page) depicts the temporal variation in oxygen isotopic signals in the three species of the foraminifera.

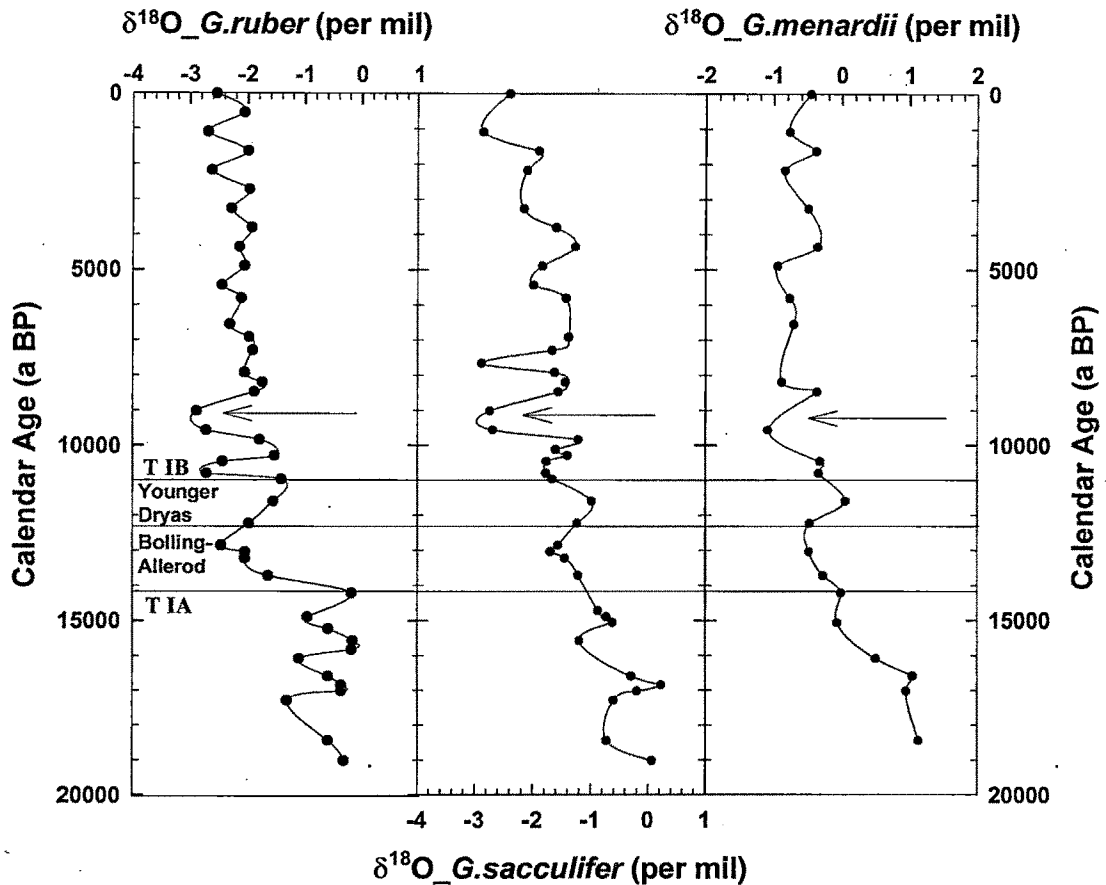


Fig.5.7. Downcore variation in $\delta^{18}\text{O}$ of three species of foraminifera in the core SS4018 G

The calcification temperature and the oxygen isotopic composition of the seawater control the $\delta^{18}\text{O}$ of the calcitic shells of foraminifera as discussed in section 2.4.1. At the present core location, processes that are controlling the oxygen isotopic value of the seawater, at the depths where the studied species dwell are the ice-volume effect and evaporation - precipitation (E - P) balance. The water temperature is controlled by the variation in the upwelling intensity that brings up cold water from deeper levels to the surface. All the three species show more or less the same signals, though a little subdued in the deeper dwelling species *G.menardii*. All the species show higher $\delta^{18}\text{O}$ values during the glacial period than the Holocene. Fairbanks (1989) calculated the global seawater oxygen isotopic curve as governed by the global ice - volume effect. It is based on the sea level curve obtained from Barbados corals

using a factor of 0.011 ‰ per meter change in sea level (Fairbanks and Matthews, 1978).

According to this curve, from LGM to T IA (Termination IA), global seawater $\delta^{18}\text{O}$ decreased by 0.25 ‰. In the core SS4018 G, $\delta^{18}\text{O}$ decrease from LGM to T IA is about 1 ‰. Remaining 0.75‰ decrease is due to seawater water temperature increase due to reduced upwelling as SW monsoon was weak upto 15 ka BP as evident from various productivity proxies discussed earlier. During the later phase of Termination IA global seawater $\delta^{18}\text{O}$ dropped by 0.3‰ (the so called melt water phase, mwp – IA). In the studied core this drop is 1.4 ‰ for *G.ruber*, 0.8 ‰ for *G.sacculifer* and 0.6 ‰ for *G.menardii*, which means that remaining decrease of 1.1 ‰, 0.5 ‰ and 0.3 ‰ respectively are due to local E – P balance. As exhibited by calcareous productivity the SW monsoon intensified at 15 ka BP resulting in enhanced winds and probably precipitation that would cause $\delta^{18}\text{O}$ values to decrease. The highest decrease is found in the surface dwelling species with the amplitude reducing in the deeper dwelling species, consistent with the above interpretation.

During Younger Dryas (13.5 ka BP to 11.5 ka BP) the $\delta^{18}\text{O}$ values increased by 1‰ for *G.ruber*, 0.8 ‰ for *G.sacculifer* and 0.6 ‰ for *G.menardii*. The global seawater $\delta^{18}\text{O}$ fell by 0.15 ‰ during this time, which means that total increase in $\delta^{18}\text{O}$ values of the foraminifera were 1.15 ‰ for *G.ruber*, 0.95 ‰ for *G.sacculifer* and 0.75 ‰ for *G.menardii*. The probable reasons for such a increase can either be enhanced upwelling or E –P balance. If it had been due to enhanced upwelling, then it should have affected all the three species equally. But the surface dwelling species shows the maximum amplitude that indicates a surface phenomenon i.e. an excess of evaporation over precipitation during that time. During Termination IB (centered at 11ka BP, mwp – IB), again $\delta^{18}\text{O}$ values decreased by ~1.2 ‰ for *G.ruber*, 0.6 ‰ for *G.sacculifer* and 0.4 ‰ for *G.menardii*. The ice – volume effect for this period is 0.2 ‰ decrease. The remaining decrease in the $\delta^{18}\text{O}$ of the foraminifera can be explained by the enhanced precipitation during that time.

Global ice – volume effect is only 0.15 ‰ from 10 – 9 ka BP. But during that period all the species exhibit a sharp reduction in $\delta^{18}\text{O}$ values by ~1 ‰ that points towards copious precipitation (enriched in lighter isotope) and hence monsoon

intensification. This observation is further corroborated by various productivity proxies viz. CaCO_3 , C_{org} and $\delta^{13}\text{C}$ in all the three species of foraminifera that exhibit a sudden enhancement centered at 10 – 9 ka BP. Further enhancement of monsoon results in increased precipitation (enriched in lighter isotope) as well as increased upwelling of colder water that shift the $\delta^{18}\text{O}$ values towards heavier (positive) side. Because of these two counter-balancing processes, the $\delta^{18}\text{O}$ values in all the foraminiferal species stay more or less uniform. Had the monsoon intensity reduced during the Holocene, the $\delta^{18}\text{O}$ should have shown a decreasing trend due to reduced upwelling. But such a decrease is not seen that indicates that SW monsoon intensity did not probably reduce during the Holocene.

In chapter 3 dealing with the core SK145-9, we have compared with the % *G.bulloides* data of the Gupta et al (2003) and inferred that the SW monsoon wind signals obtained in the western Arabian Sea cores are in good agreement with the SW monsoon runoff signals obtained from the eastern Arabian Sea cores. This inference is based on the observation that % *G.bulloides* decline is accompanied by reduced precipitation. But in this chapter, % *G.bulloides* (which is a manifestation of calcareous productivity) decline is attributed to increasing monsoon. It can be explained if we take **thresholds in the response** of % *G. bulloides* or the CaCO_3 % in to account. When the abundance of *G. bulloides* was ~28%, further intensification of monsoon brought it down due to reasons discussed earlier in this chapter. However, in the Chapter-3, the values were already low (~10%). Here the intensification of the monsoon may increase rather than decrease the abundance.

5.6. Spectral Analysis:

The periodicities in the time-series data of various proxies has been determined using the REDFIT 3.6 program (Schulz and Mudelsee, 2002). The power spectra obtained for various proxies are given in the Fig.5.7. Out of the productivity proxies, $\delta^{13}\text{C}$ in *G.sacculifer* exhibits a dominant periodicity of ~25,600 years (y), which probably corresponds to the precessional cycle of the earth (~23 kyr) seen by

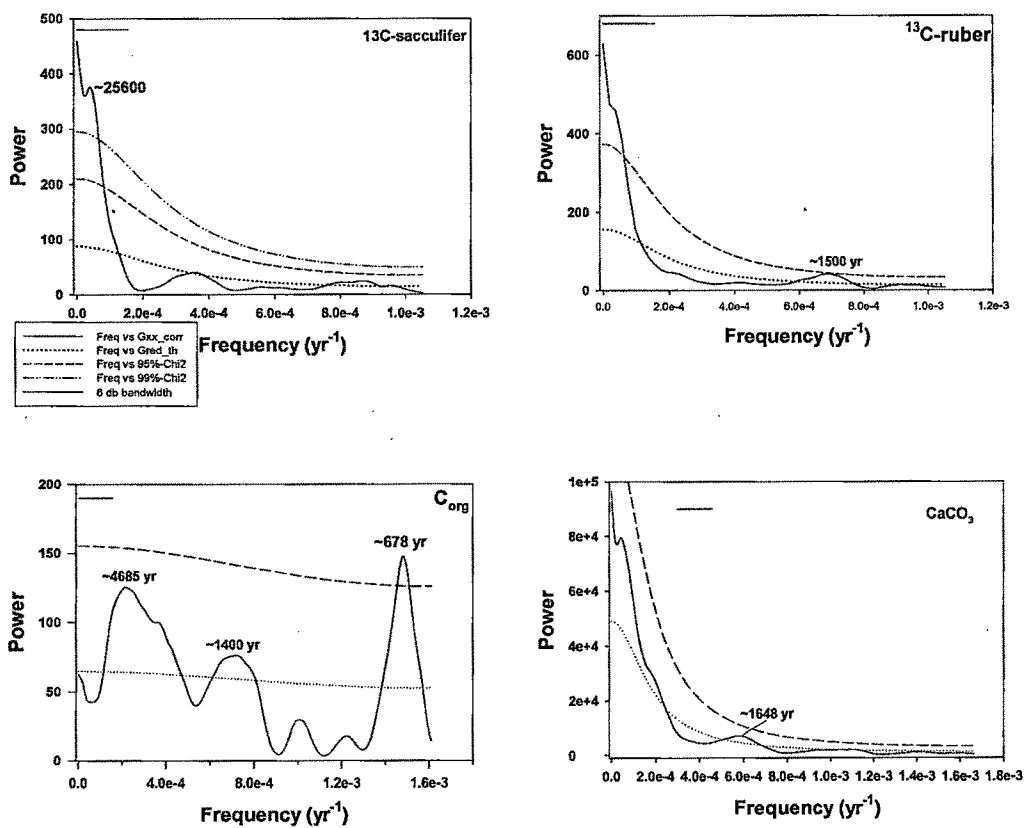
other workers (e.g. Clemens et al, 1991, Leuschner and Sirocko, 2003) in sediment cores from the western Arabian Sea and northern Arabian Sea (Reichart et al, 1997).

Other productivity proxies like $\delta^{13}\text{C}$ in *G.ruber*, C_{org} and CaCO_3 exhibit periodicities of ~1500 y, 1392 y and 1648 y respectively, which are although below the 95% confidence limit but are still above the background. These periodicities are very close to the widely reported 1470 ± 500 y periodicity from various archives (e.g. Bond et al, 1997; Sirocko et al, 1996; Schulz et al, 1998; Mayewski et al, 1998, Campbell et al, 1998; Sarkar et al, 2000 Agnihotri et al, 2003b). The 1470 y cyclicity is exhibited by the Dansgaard–Oeschger interstadials (Grootes and Stuiver, 1997) implying the correlation between low latitude monsoon variations and high latitude changes. $\delta^{18}\text{O}$ in *G.ruber* and *G.sacculifer* also exhibit 1370 y periodicity that is below the 95% confidence limit. The probable reason for these proxies to fall below the 95% confidence limit is the poor temporal resolution which on average is ~500 y except in the case of C_{org} and CaCO_3 where it is ~300 y. Moreover, the $\delta^{18}\text{O}$ values are controlled by many processes such as SST, salinity etc. leading to suppression of the amplitude of frequencies. C_{org} further demonstrate a dominant frequency of ~678 y (above 95% confidence limit) that corresponds very well to ~700 y periodicity seen by Sarkar et al (2000) in the $\delta^{18}\text{O}$ of the planktonic foraminifera (*G.sacculifer*) and Agnihotri et al (2003) in productivity related elements in the sediment cores from the eastern Arabian Sea. Furthermore, Wang et al (1999) report a periodicity of ~775 y from a sediment core from the South China Sea that is being influenced by SE Asian monsoon. These common frequencies might point towards the common forcing factor.

Another productivity indicator $\delta^{15}\text{N}$ exhibit a dominant frequency of ~1982 y that is above even the 99% confidence level. Similar periodicities of ~2028 y and ~2200 y are exhibited by $\delta^{18}\text{O}$ in *G.ruber* and *G.sacculifer* respectively, albeit below the 95% confidence limit due to the reasons discussed earlier. Similar periodicity of 2200 y has been observed by Naidu and Malmgren (1995) in upwelling intensity indices from a core from the Oman margin, Western Arabian Sea. Furthermore, a 2300 y cyclicity (Magny, 1993; Sonnet and Finney, 1990) and a 2050 y periodicity (Damon and Peristykh, 2000) are reported for the atmospheric ^{14}C variations. Based on similar periodicity for oceanic proxy and the ^{14}C variations, Naidu and Malmgren

(1995) proposed that oceanic circulation changes are controlling the ^{14}C periodicities at 2300 y time scale as enhanced oceanic circulation will induce greater vertical circulation that will release ^{14}C depleted CO_2 into the atmosphere. They further argue that thermohaline circulation might influence the Asian monsoon through various complex feedback mechanisms as Street - Perrott and Perrott (1990) have reported the influence of deep-sea circulation on precipitation over northern tropical areas. Our multi-proxy study appears to reinforce the above hypothesis.

$\delta^{18}\text{O}$ and $\delta^{13}\text{C}$ (not shown in the Fig.5.7) in *G.menardii* do not show any significant periodicity, probably due to a coarser sampling resolution (~ 800 y).



Contd...

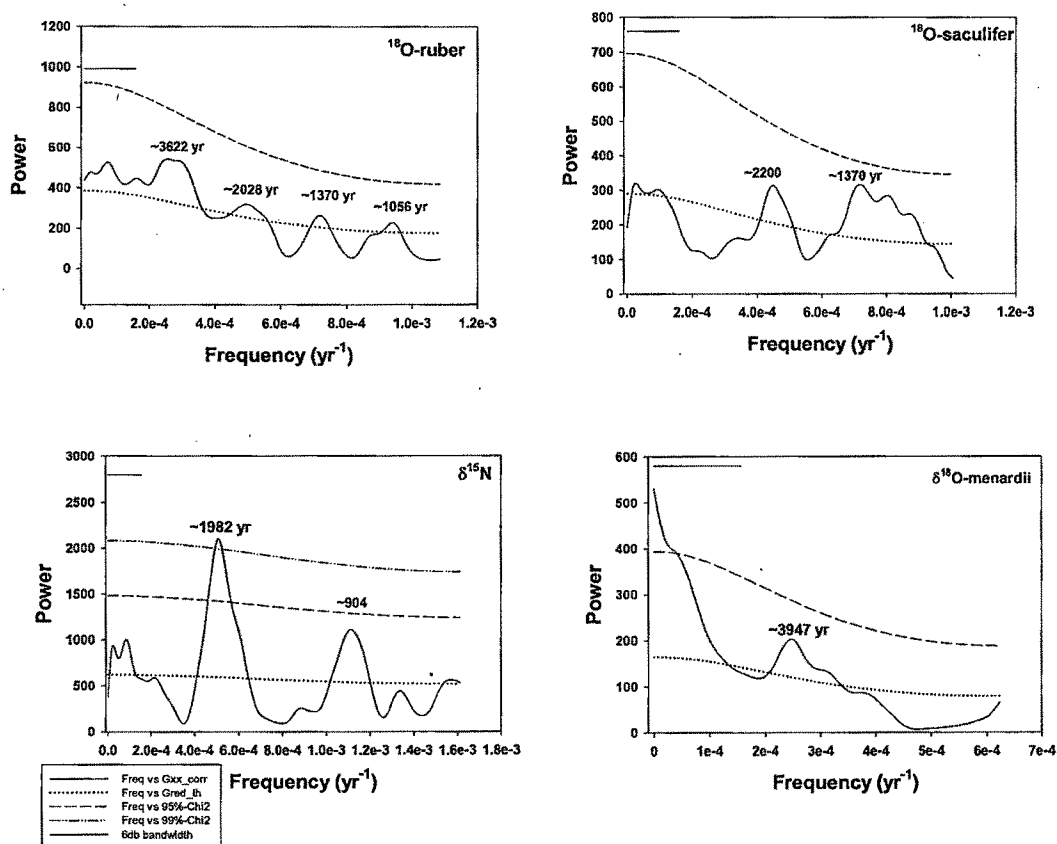


Fig.5.8. Power spectra for various paleoclimatic proxies. Horizontal line at the upper left-hand corner represents 6db bandwidth of the spectral resolution. Gxx_corr denotes amplitude or power of various frequencies; Gred_th shown by dotted line is the background signal; dashed line and dash-dot-dot line denote the 95% and 99% significance levels calculated using the χ^2 test.

5.7. Inferences:

- i. The southwest monsoon was weaker during the early deglacial period as evident from the calcareous productivity and supported by organic productivity (C_{org} and $\delta^{13}C$) and $\delta^{18}O$ analysis carried out on three different species of planktonic foraminifera.
- ii. A sudden intensification of SW monsoon is observed centered at ~14.5 ka BP. It coincides with the first step of deglaciation (T IA) and such a rapid response by the monsoon system can be attributed to albedo changes over central Asia and Tibetan plateau that would enhance the land – sea air pressure difference during summer.
- iii. Monsoon intensity seems to decline during the younger Dryas as evident by excess of evaporation over precipitation. The monsoon again regained its strength during the T IB (centered at 11 ka BP).
- iv. At ~9 ka BP, another episode of monsoon intensification took place just after the maximum tropical summer insolation at 10 ka BP between $20^{\circ}N$ and $35^{\circ}N$.
- v. Thereafter SW monsoon strengthened during the Holocene as observed in the multi-proxy isotopic and chemical data. Monsoon does not appear to have decreased during the Holocene as proposed by some earlier studies in this region.
- vi. Spectral analysis points that on Milankovitch timescale, monsoon is mainly influenced by the precessional cycle of the earth. On shorter timescales the dominant periodicities exhibited by monsoon are

~1400y and 700 y that points towards the correlation with high latitude and thermohaline circulation changes.